https://doi.org/10.2352/issn.2168-3204.2025.22.1.33

From Negatives to Positives: Modeling the Photochemical Printing Process

Giorgio Trumpy; Norwegian University of Science and Technology (NTNU); Gjøvik, Norway
Ottar A. B. Anderson; Intermunicipal archive of Møre og Romsdal (IKAMR); Ålesund, Norway

Abstract

Most analog color photographs were captured on film negatives. This study presents a scientifically validated workflow for digitizing and inverting color negatives to produce digital positives that closely emulate traditional enlarger prints. A custom imaging system with narrow spectral bands, designed to match the spectral sensitivities of photographic paper, was tested against a conventional digitization method. Final color images were computed based on the spectral densities of the paper's image-forming dyes, simulating the photochemical printing process. Results demonstrate that aligning digitization spectral bands with photographic paper characteristics improves inversion accuracy. This research lays the foundation for enhanced archival preservation of color negatives and provides a method for generating digital positives that closely match the aesthetic of original prints.

Motivation

The widespread success of color photography is largely attributed to the negative-positive process. In fact, the vast majority of photographs were historically captured on color negatives [10]. Positive prints from these negatives were traditionally produced using enlargers. Today, billions of color negatives are held in archives and private collections worldwide, often without corresponding prints. A common preservation approach is to digitize the negatives and use image processing techniques to invert them into positive images. While tools like *Negative Lab Pro* and *FilmLab* facilitate this process, research into optimizing both the image capture and processing workflows remains limited. Notably, few efforts have focused on achieving digital results that faithfully replicate the look and tonal qualities of traditional enlarger prints, though some promising experimental approaches have recently emerged [5].

Problem

This study addresses two key questions: (1) Can the photochemical printing process be effectively modeled? (2) Are specific spectral bands for the digital capture of negatives advantageous in producing higher-quality digital positives?

Approach

A set of film negatives and their corresponding paper prints were selected for testing. This collection has been preserved according to standard archival recommendations throughout its 30-year lifespan (30-50% RH, 21°C or lower, light-tight storage). The paper prints were digitized using a Phase One iXG 100 MP camera with a Schneider Kreuznach RS 72mm f/5.6 lens and a Phase One D8 R+ LED light source. The setup complied with ISO 19264-1 specification level A, utilizing the ISA Object Level Target and the Phase One NimbusQA cloud-based service for verification. The film negatives were digitized using two different imaging systems:

1. **Broad-band system**: Phase One XF IQ4 150 MP camera with a Schneider Kreuznach Blue Ring AF 120mm f/4 Macro lens and a KAISER Prolite LED 50/37 light source.
2. **Narrow-band system #1**: QHY600 monochrome camera with a Tokina atx-i 100mm f/2.8 FF Macro lens, and a THOUSLITE LEDCube light source.

Each system produced RGB images corresponding to a different set of spectral bands. In the broad-band system, the spectral bands were primarily determined by the sensor's sensitivities, which exhibit significant spectral overlap. In contrast, the narrow-band system's spectral bands were defined by the emission characteristics of the light source. For the narrow-band system, RGB images were built from three sequential monochrome captures, with the LEDCube's emission tuned to match the spectral sensitivities of the photographic paper used for the prints. This approach aimed to digitally replicate the photochemical printing process.

For the experimental validation, the positive prints were manually created using a DURST Laborator 1200 CLS 501 enlarger on Kodak Ektacolor Supra II gloss paper [4], processed with RA4. To match the paper's spectral response, the THOUSLITE LEDCube channels were adjusted accordingly. The match was satisfactory for red and blue wavelengths, but a significant mismatch occurred in the green region (see Fig. 1). This mismatch is due to the 'yellow-green gap', where limited options exist for narrow-band LEDs in the 530–590 nm range [9].

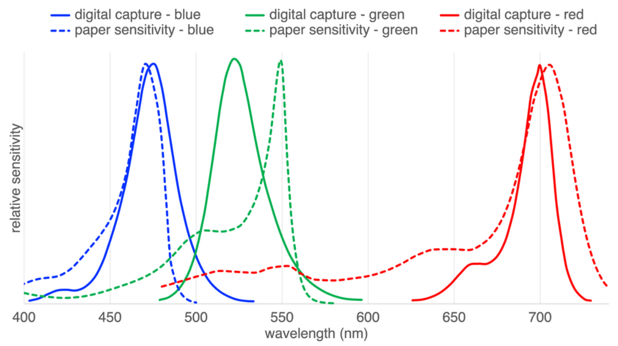

Figure 1*. Comparison between the spectral sensitivity of the blue-, green- and red-sensitive layers of Kodak Ektacolor Supra II gloss paper and the spectral sensitivities of the "narrow-band system #1".*

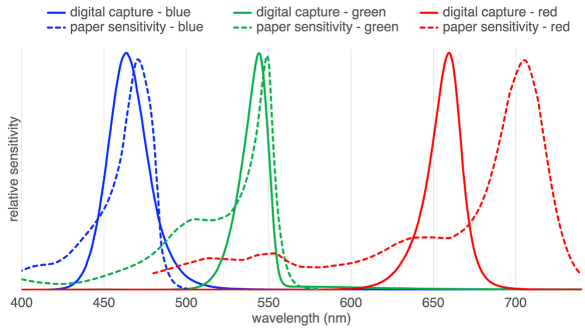

Figure 2. Comparison between *the* spectral sensitivity of the blue-, green- and red-sensitive layers of Kodak Ektacolor Supra II gloss paper and the spectral sensitivities of the "narrow-band system #2".

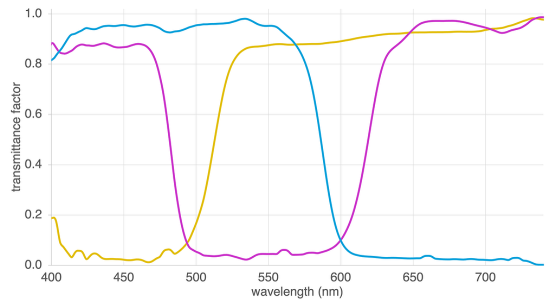

Figure 3*. Enlarger DURST M670 COLOR. Transmittance factor of fully engaged yellow, magenta and cyan filters measured with SEKONIC Spectrometer C-800.*

To overcome the mismatch between the green curves in Figure 1, a third imaging system was introduced:

3. **Narrow-band system #2**: QHY600 monochrome camera with a Canon MP-E 65mm f/2.8 1–5x Macro lens and a custom multichannel illumination with LEDs and interference filters.

As detailed in a previous publication [8], this imaging system incorporates narrow-band channels in the 530–590 nm range by filtering a broad-band LED source through interference filters. To approximate the paper's spectral sensitivities, three channels were selected from the custom illuminator. This configuration achieved a good match for the blue and green channels. However, the red channel peaked approximately 50 nm short of the red-sensitive layer of the photographic paper, which has its maximum sensitivity shifted toward the deep red, around 710 nm (see Fig. 2). This particularly long-wavelength sensitivity was intentionally introduced by the paper manufacturer to enable handling and printing under amber safelights in the darkroom. In our current imaging setup, it was not possible to reproduce this deep-red sensitivity due to limitations in the available light source. Nonetheless, this discrepancy is not expected to have a significant impact, as the spectral absorption characteristics of color negative film are relatively flat between 660 nm and 710 nm, minimizing potential differences in the resulting digital image.

The transmittance values in the digital images captured from the film negative with the narrow-band system (T_{NEG}) were directly related to the exposure responsible for generating the image-forming dyes with the RA4 process. Based on the spectral densities of the image-forming dyes in the photographic paper (OD_{IFD}) [4], a spectral cube (R_{print}) was computed using the following equation:

$$R_{print} = T^R_{NEG} \cdot OD^C_{IFD}(\lambda) + T^G_{NEG} \cdot OD^M_{IFD}(\lambda) + T^B_{NEG} \cdot OD^Y_{IFD}(\lambda) \quad (1)$$

R_{print} contains absorbance values at 5 nm intervals within the 400-700 nm range, providing an initial approximation of the paper print's reflection properties. In accordance with the principles of the photographic process, the red-sensitive layer forms the cyan dye, the green-sensitive layer forms the magenta dye, and the blue-sensitive layer forms the yellow dye.

Leveraging the psychophysical characteristics of the human visual system, the final aesthetic of the positive image is calculated from the R_{print} cube performing colorimetric calculations that consider the standard observer [7]. For each pixel in the R_{print} spectral cube, the tristimulus values are obtained using the following summation:

$$\begin{bmatrix} X \\ Y \\ Z \end{bmatrix} = \sum_\lambda D50 \cdot 10^{-R_{print}} \cdot CMFs \quad (2)$$

where D50 is the spectral emission of the standard illuminant, and CMFs are the CIE 1931 2° color matching functions [2].

To produce a conveniently readable image file, the resulting tristimulus values are scaled and converted to RGB values considering the Adobe RGB standard color space [3].

It is important to note that the resulting color image should be considered an initial approximation rather than a definitive reproduction of the chromogenic print. The current calculation does not take into account several key variables that affect the final print appearance, including the CMY filtration settings of the enlarger head, the exposure level, and the non-linear response (characteristic curves) of the photographic paper. The CMY filtration system operates using subtractive filters arranged in series, with their individual transmittance characteristics shown in Figure 3. Despite these limitations, the method described here provides a solid foundation for producing digital positives that closely emulate the visual qualities of traditional chromogenic prints. Minor adjustments—guided by reference prints or expert judgment—can be applied to fine-tune the image to match the intended aesthetic outcome.

Results

This paper presents the result of the method for two 120-format negatives taken on a roll of Agfa Optima 125, which were used to test the narrow-band system #1 (Figs. 4 and 5). In addition, two 135-format negatives, one taken on a roll of Agfa Optima 125 and one on Kodak Gold 200, were used to test the narrow-band system #2 (Figs. 6 and 7). The corresponding paper prints were created on Kodak Ektacolor Supra II gloss paper (Figs. 4 to 7 - center). The film negatives were captured both with the broad- and the narrow-band systems (described in the previous section). The experiments were conducted with the intent to verify that mimicking the spectral sensitivities of the photographic paper used for printing (Fig. 1 and 2) actually provides a better result.

Linear images expressing transmittance values were used as input (Figs. 4 to 7 - top), considering the unexposed part as the white reference, thus counterbalancing the orange correction mask. Hence, the normalized digital numbers in the RGB channels of the digitized

Figure 4. Motive 1 – "Man standing on beach". Left: Narrow-band workflow. Center: Paper print. Right: Broad-band workflow. At the sides, from top to bottom, the linear images with whitepoint on the orange mask (input), the results of Eqs. 1 and 2 (inverted), and the results of the 1D-LUTs. Photo credit: Ottar A.B. Anderson. Digitized by Giorgio Trumpy and Piotr Cabaj.

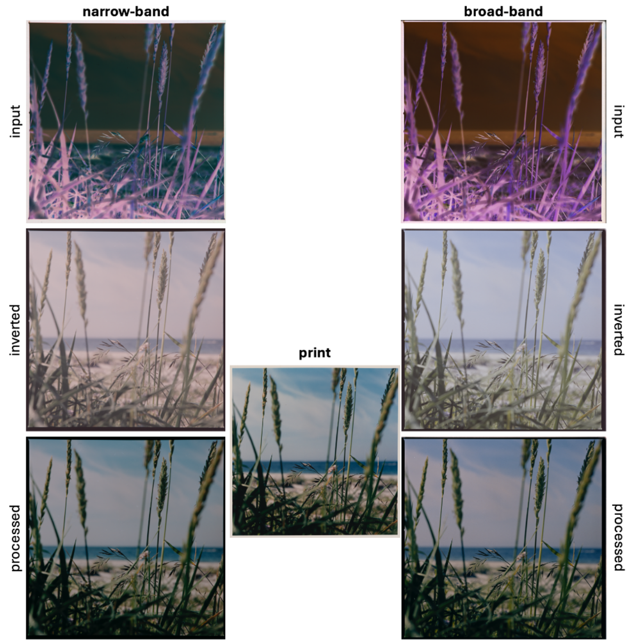

Figure 5. Motive 2 – "Straw on beach". Left: Narrow-band workflow. Center: Paper print. Right: Broad-band workflow. At the sides, from top to bottom, the linear images with whitepoint on the orange mask (input), the results of Eqs. 1 and 2 (inverted), and the results of the 1D-LUTs. Photo credit: Ottar A.B. Anderson. Digitized by Giorgio Trumpy and Piotr Cabaj.

negatives represent the T_{NEG} values in Eq. 1, while the OD_{IFD} spectra are obtained from the photo-paper's datasheet [4].

The inversion process represented by Eqs. 1 and 2 produced an approximation of the positive image (Figs. 4 to 7 - center).

To account for the CMY settings of the enlarger head, the exposure level, and the characteristic curves of the paper, additional image processing was applied using one-dimensional lookup tables (1D-LUTs). Specifically, color differences between the digitized paper print and the inverted images were minimized.

After an initial feature-based image registration [1], the image to be color corrected is processed with three curves for the R, G and B channels.

Each curve is defined by four nodal points (the black and the white points plus two midpoints). The process finds the optimal position of the nodal points through a multistep minimization process based on the Nelder-Mead simplex algorithm [6]. The results are presented at the bottom of Figs. 4 to 7.

Narrow-band system #1 – 120-format negatives

- Motive 1 (Fig. 4): The images produced after the final color correction differ primarily in skin tone, sky, and seawater. The broad-band workflow introduced an unnatural reddish cast to the sky and sea foam. While the narrow-band workflow does not perfectly match the print's colors, the resulting image appears more natural.
- Motive 2 (Fig. 5): Neither workflow fully captures the deep blue of the sea water as seen in the print. However, when comparing the results to the print, the narrow-band workflow produces a closer match for the sky's color.

Narrow-band system #2 – 135-format negatives

- Motive 3 (Fig. 6): The results of the two workflows differ mostly in the blue tones, with the broad-band workflow exhibiting an excessive blue component, which is visible in the background landscape and in some rooftops. The narrow-band version aligned more closely with the print.
- Motive 4 (Fig. 7): Neither workflow accurately captures the red of the cat's tongue as seen in the print. However, the narrow-band workflow produces a closer match.

Conclusions

Our experiments demonstrate that selecting spectral bands for digitizing negatives to align with the spectral sensitivities of photographic paper positively impacts the inversion process. Additionally, modeling the photochemical printing process using data from the photographic paper's datasheet, as represented by Eqs. 1 and 2, yields convincing results.

Further studies are necessary to validate these findings by testing additional examples and comparing our method with existing market tools.

References

[1] Bay, H. *et al.* (2008) 'Speeded-Up Robust Features (SURF)', *Comput. Vis. Image Underst.*, 110(3), pp. 346–359.

[2] CIE (2019) *Colorimetry — Part 1: CIE standard colorimetric observers*. ISO standard ISO/CIE 11664-1:2019. CIE International Commission on Illumination.

[3] ISO (2011) *Graphic technology — Prepress digital data exchange — Part 4: Wide gamut display-referred standard colour image data [Adobe RGB (1998)/SCID]*. ISO standard ISO 12640-4:2011.

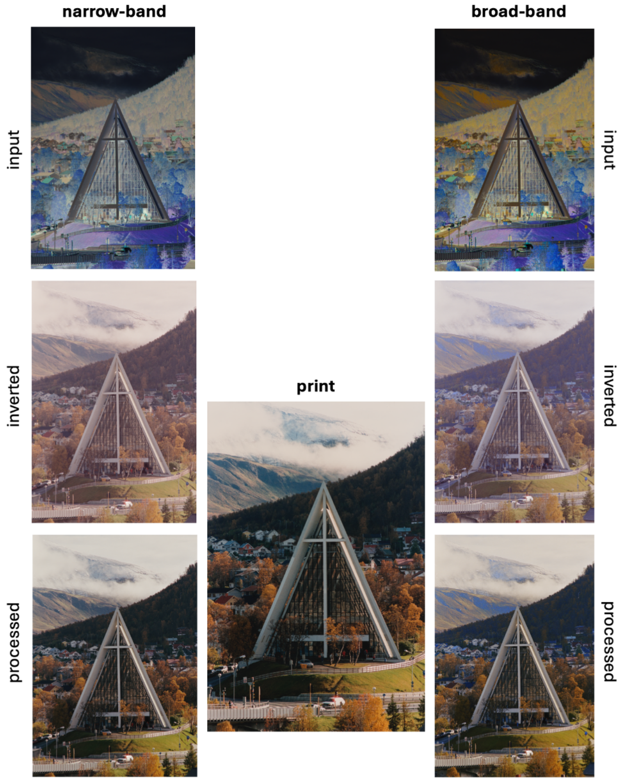

Figure 6. *Motive 3 – "The Arctic Cathedral in Tromsø". Left: Narrow-band workflow. Center: Paper print. Right: Broad-band workflow. At the sides, from top to bottom, the linear images with whitepoint on the orange mask (input), the results of Eqs. 1 and 2 (inverted), and the results of the 1D-LUTs. Photo credit: Ottar A.B. Anderson. Digitized by Giorgio Trumpy and Piotr Cabaj.*

Figure 7. *Motive 4 – "Cat yawning". Left: Narrow-band workflow. Center: Paper print. Right: Broad-band workflow. At the sides, from top to bottom, the linear images with whitepoint on the orange mask (input), the results of Eqs. 1 and 2 (inverted), and the results of the 1D-LUTs. Photo credit: Ottar A.B. Anderson. Digitized by Giorgio Trumpy and Piotr Cabaj.*

[4] Kodak (2022) *KODAK PROFESSIONAL SUPRA III Paper*. Technical data E-141.

[5] Koraks tinkers, 2024. Perfecting primaries – Another look at LED wavelengths for RA4 paper – Koraks tinkers. URL https://tinker.koraks.nl/photography/perfecting-primaries-another-look-at-led-wavelengths-for-ra4-paper/ (accessed 5.14.25).

[6] Lagarias, J.C. *et al.* (1998) 'Convergence Properties of the Nelder-Mead Simplex Method in Low Dimensions', *SIAM J. Optim.*, 9(1), pp. 112–147.

[7] Schanda, J. (2007) 'CIE Colorimetry', in J. Schanda (ed.) *Colorimetry. Understanding the CIE System*. 1st edn. Vienna, Austria : Hoboken, N.J: Wiley-Interscience.

[8] Trumpy, G., et al (2021) 'A Multispectral Design for a New Generation of Film Scanners', in: Proc. SPIE 11784.

[9] Usman, M. *et al.* (2021) 'Green gap in GaN-based light-emitting diodes: in perspective', *Critical Reviews in Solid State and Materials Sciences*, 46(5), pp. 450–467.

[10] Wolf, H. (1997) *Marketingplan zur Neueinführung des Filmsystems APS für ein Unternehmen der Fotoindustrie*. Diplomarbeit. Fachhochschule Köln.

Author Biography

Giorgio Trumpy is currently Associate Professor in Color Imaging at the Norwegian University of Science and Technology and founding member of Scan2Screeen GmbH (Swiss company for film digitization). Imaging Scientist with experience in bridging the gap between art and science. Fields of expertise span from optics to spectroscopy, from colorimetry to image processing, from heritage conservation to visual arts. Previously worked at the Institute of Applied Physics in Florence on non-invasive analyses of paintings with fiber optic reflectance spectroscopy and hyper-spectral reflectance imaging (2006-2010). PhD project at the University of Basel (2010-2013), devising an optical setup for the detection and restoration of dust and scratches on photographs and motion-picture films. Postdoc fellow at National Gallery of Art in Washington DC (2014-2016), designing spectral imaging methodologies for works of art. Research scientist at the University of Zurich (2016-2022) conducting scientific analyses of historical film colors and designing an innovative archival film scanner.

Ottar A.B. Anderson is Head of Photography at Intermunicipal archive of Møre og Romsdal (IKAMR). Interested in the technical part of photography, metadata and new technology developments within cultural heritage imaging and digital publishing platforms. Former photography background from the Royal Norwegian Air Force and Kodak Q-lab photo technician for professional photographers, with hands-on extended understanding of the photographic RA-4/R3 print- and C-41 film development processes. Member of the expert working group ISO/TC 42 JWG 26 – "Imaging system capability qualification for archival recording and approval" and The Digital Object Authenticity Working Group (DOAWG)